Supporting Information

Prussian Blue Analogue Derived from Leather Waste as Bifunctional Catalyst in Zinc-Air Batteries

Meng-yu Liu[a], Shi-yi Shen[a], Jia-hua Guo[a], Ze-yu Zhu[b], Bao-li Zha[b], Jiansheng Wu[b]*, Wen-Bo Pei[a]*, Xiao-Ming Ren[a], Fengwei Huo[b]

[a] School of Chemistry and Molecular Engineering, Nanjing Tech University, Nanjing 211816, China.

[b] Key Laboratory of Flexible Electronics (KLOFE), School of Flexible Electronics (Future Technologies), Institute of Advanced Materials (IAM), Nanjing Tech University, 30 South Puzhu Road, Nanjing 211816, China.

*Corresponding author: Jiansheng Wu, Wen-Bo Pei

Key Laboratory of Flexible Electronics (KLOFE), School of Flexible Electronics (Future Technologies), Institute of Advanced Materials (IAM), Nanjing Tech University, 30 South Puzhu Road, Nanjing 211816, China

School of Chemistry and Molecular Engineering, Nanjing Tech University, Nanjing 211816, China.

E-mail: iamjswu@njtech.edu.cn; iamwbpei@njtech.edu.cn

Experimental

$Co(NO_3)_2 \cdot 6H_2O$, sodium hydroxide, potassium hydroxide, hydrochloric acid and $Zn(CH_3COO)_2$ were purchased from Aladdin. Leather waste was the leftover material produced in the leather production process purchased from Xinghao Leather Factory. Nafion (5 wt%) was purchased from Sigma Aldrich. GO was purchased from Shenzhen Suiheng Technology Co., Ltd. All the chemicals were purchased and used directly without any further purification. Commercial Pt/C and RuO_2 were purchased from Suzhou Sinero Technology Co., Ltd. Deionized water (DI water) was homemade by our laboratory.

Leather waste was first rinsed with DI water and dried in an oven to remove moisture. The dried leather was then crushed into flocculent matter by a crusher. The crushed leather (1g) was added to a 20 mL NaOH solution (0.2M) and stirred at 90℃ for a duration of 6 hours. Next, $Co(NO_3)_2 \cdot 6H_2O$ was dissolved in 5 mL DI water and sonicated for 20 minutes to form solution A, while GO (10 mg) was dissolved in 15 mL DI water through sonication to form solution B. Solution A was added first, followed by the addition of solution B while still hot. The mixture was stirred at 90 °C for 2 hours, gradually cooled down to room temperature, and stirred for an additional 12 hours before being freeze-dried in a freeze dryer over 24 hours. The material was then heated in a tubular furnace at 5 °C min^{-1} up to 200 °C under an air atmosphere for 30 minutes and allowed to naturally cool to room temperature. Subsequently, the material was heated again at 5 °C min^{-1} up to 700 °C under an argon atmosphere for 2 hours and naturally cooled back down to room temperature. Afterward, the material was ground, washed with 10% HCl at 80 °C for 8 hours, filtered, and rinsed with DI water before being dried in a vacuum drying oven at 60 °C for 12 hours.

Material characterization

Powder X-ray diffraction (PXRD) measurements were performed using a Smart Lab 3 KW instrument with Cu Kα radiation source (λ=1.5418 Å), over the range of 10° to 80°. Fourier transform infrared (FT-IR) spectra were measured using INVENIO-S. Raman spectra were collected on a WITec Alpha 300R confocal Raman microscope. Specific surface area and pore size distribution tests were carried out using a Brunauer-

Emmett-Teller system (BET). Scanning electron microscopy (SEM) imaging, coupled with energy-dispersive X-ray spectroscopy (EDS), was performed using a FEI Quanta FEG 250 field emission scanning electron microscope.

Electrochemical measurements

In the standard three-electrode system (PINE Wave Driver 20), the catalytic properties of six different samples, namely LWCA-Co-600, LWCA-Co-700, LWCA-Co-800, LWCA-Co-900, Pt/C and RuO_2 were investigated for oxygen reduction reaction (ORR) and oxygen evolution reaction (OER) at room temperature. A glassy carbon rotating disk electrode (RDE) with a diameter of 5 mm and a surface area of 0.196 cm^2 was meticulously polished and thoroughly cleaned using alumina particles of varying sizes (1.0 μm, 0.5 μm and 0.03 μm).

The glass carbon RDE was used as the working electrode, Hg/HgO electrode as the reference electrode, and carbon rod as the opposite electrode. The working electrode ink was prepared as follows: taking 5 mg LWCA-Co-700 sample, adding 780 μL ethanol, 200 μL DI water and 20 μL 5% Nafion solution to form a uniform mixed sample by ultrasonication. This mixture underwent ultrasonic dispersion in an ice-water bath for 30 minutes to achieve uniformity. Subsequently, 10 μL of the evenly dispersed ink was drop-casted onto the glassy carbon electrode and allowed to air-dry at room temperature, resulting in the formation of a uniformly dispersed catalyst layer. The catalyst loading on the glassy carbon electrode amounted to approximately 0.1 mg cm^{-2}.

Oxygen was introduced into the electrolyte for a duration of 30 minutes to achieve oxygen saturation prior to testing. Linear sweep voltammetry (LSV) was utilized to measure ORR, employing a scan rate of 10 mV s^{-1} within the potential range of −0.8 to 0.1 V during the positive scan. For OER, LSV measurements were conducted at a scan rate of 10 mV s^{-1} within the potential range of 0.1 to 1.0 V during the positive scan. Polarization tests were performed at various rotational speeds ranging from 400 to 2500 rpm using LSV with a scan rate of 10 mV s^{-1}. The electron transfer number (n) was calculated using Koutecky-Levich Equations.

$$\frac{1}{J}=\frac{1}{J_K}+\frac{1}{J_L}=\frac{1}{B\omega 0.5Jk} \quad (1)$$

$$B=0.2nFC_0D_0^{2/3}V^{-1/6} \quad (2)$$

Where J is the measured current density (mA cm^{-2}), J_k is the kinetic current density (mA cm^{-2}), J_L is the limiting current density (mA cm^{-2}), ω represents the angular velocity (rpm), F is the Faraday constant (96485 C mol^{-1}); C_0 stands for the bulk concentration of O_2 (1.2×10^{-6} mol cm^{-3}), D_0 is the O_2 diffusion coefficient (1.9×10^{-5} cm^2 s^{-1}) in 0.1 M KOH, and V denotes the kinetic viscosity of 0.1 M KOH (0.01 cm^2 s^{-1}).

Fabrication of liquid-state Zinc-air batteries

The liquid Zinc-air battery was constructed using a customized mold with an effective area of approximately 1.766 cm^{-2}. To create a homogeneous catalyst ink, a mixture of 25 mg LWCA-Co-700 sample and 6.25 conductive carbon black (super P) was dispersed in 900 μL ethanol and combined with 100 μL of Nafion solution containing 5% concentration. The resulting mixture underwent ultrasonic treatment for 30 minutes followed by stirring at room temperature for 12 hours. Subsequently, the catalyst ink was sprayed onto a hydrophobic carbon paper measuring 2 cm × 2 cm and subjected to vacuum drying at 60 °C for five hours, serving as the air cathode for the zinc-air battery.

To compare the performances, a mixture of Pt/C (20%) and RuO_2 (1:1) was prepared by dispersing them in a solution containing ethanol and Nafion in the same ratio as mentioned earlier. Alkaline electrolyte solutions were prepared using 6 M KOH + 0.2 M $Zn(Ac)_2 \cdot H_2O$. A polished zinc foil with a thickness of four millimeters was used as the negative electrode, while copper foil served as the conductor. The aforementioned positive electrode materials were assembled into zinc-air batteries.

Polarization curves and corresponding power density measurements were conducted on an electrochemical workstation (CHI660E). Charging and discharging tests were performed on a battery tester (NEWARE) at room temperature.

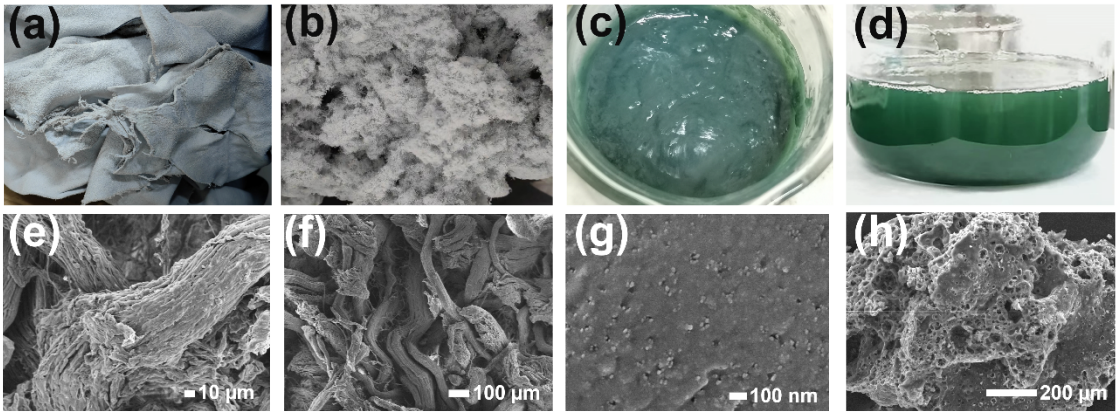

Fig. S1. The various processes of leather include (a) raw materials that have not been cleaned, (b) leather after crushing, (c) leather during the heating and dissolving process, and (d) the final solution after leather dissolution. Additionally, SEM images depict (e)(f) rawhide, (g) freeze-dried samples, and (h) LWCA-Co-700

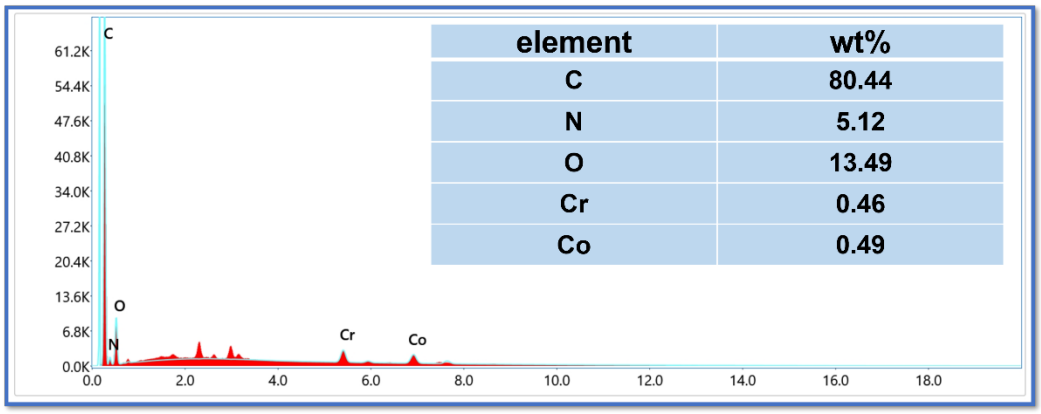

element	wt%
C	80.44
N	5.12
O	13.49
Cr	0.46
Co	0.49

Fig. S2. Element content for C, N, O, Cr, Co of LWCA-Co-700.

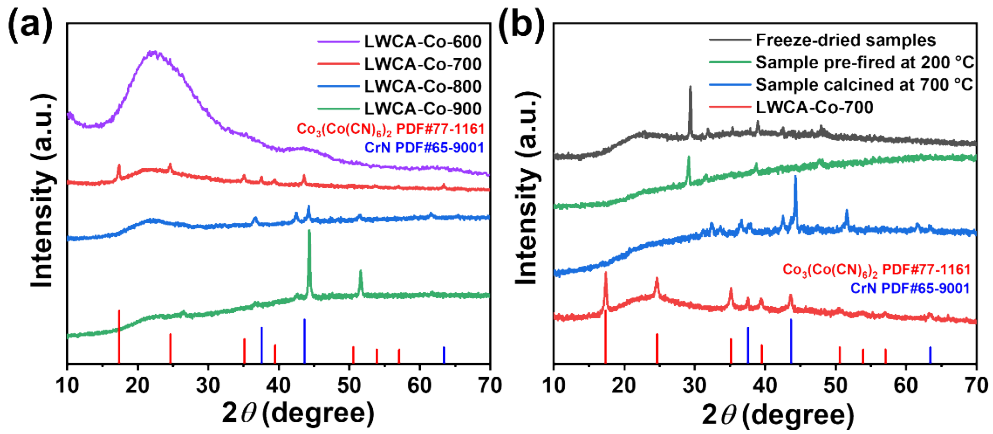

Fig. S3. (a) XRD patterns for LWCA-x, (b) freeze-dried samples, pre-fired samples at 200 °C, calcined samples at 700 °C, and LWCA-Co-700.

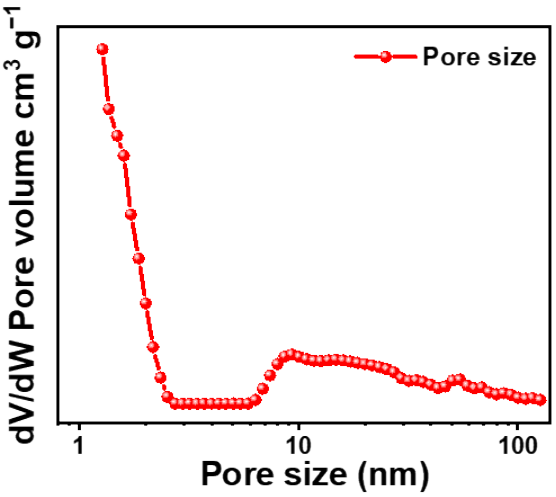

Fig. S4. Pore size distribution of LWCA-Co-700.

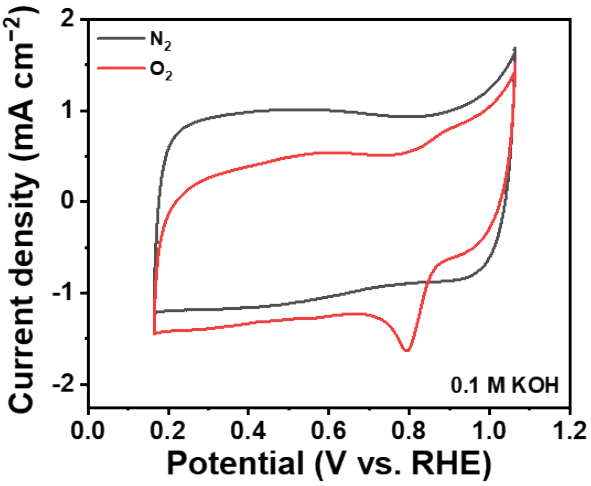

Fig. S5. CV curves of LWCA-Co-700 in N_2 and O_2 saturated 0.1 M KOH solution.

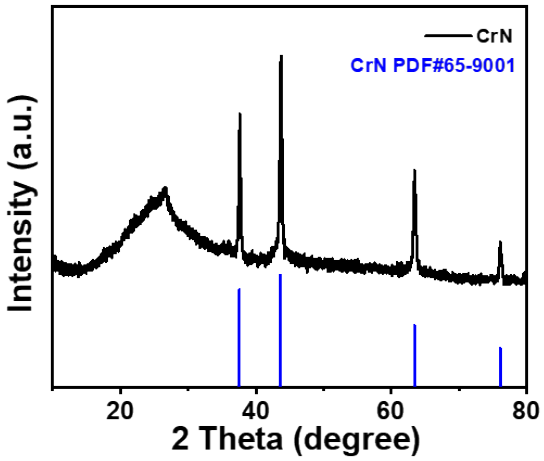

Fig. S6. Powder XRD pattern of the as-prepared CrN sample.

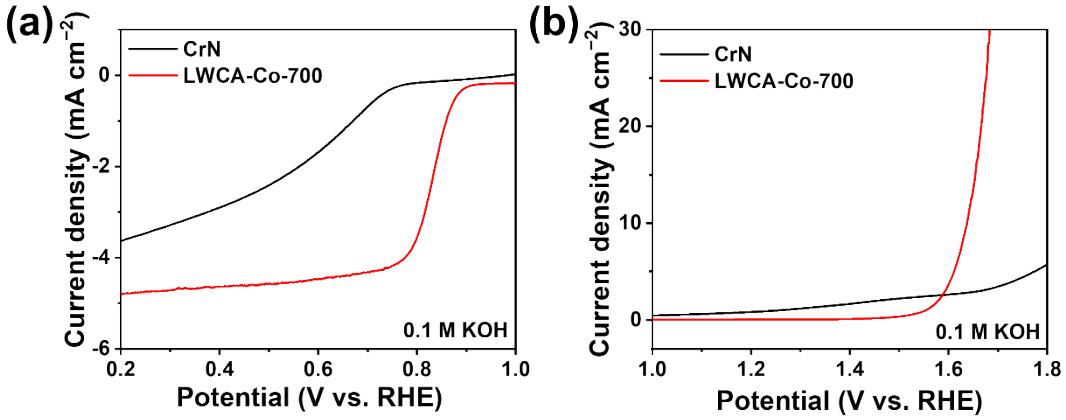

Fig. S7. (a) Rotational speed of 0.1 M KOH solution at O_2 saturation is measured to be 1600 rpm. LWCA-Co-700 and CrN exhibit contrasting polarization curves for ORR. (b) Contrasting polarization curves observed for OER.

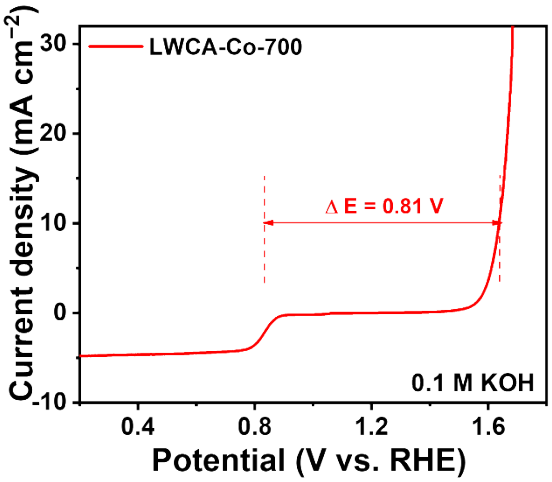

Fig. S8. LSV profiles of the LWCA-Co-700 for bifunctional performance evaluation.

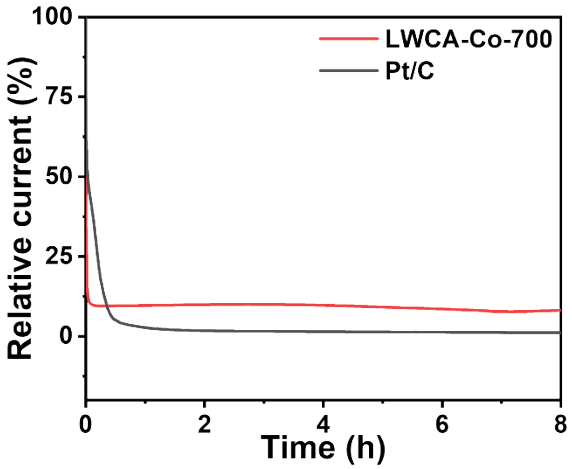

Fig. S9. Stability test in 0.1 M KOH solution of LWCA-Co-700 and Pt/C.

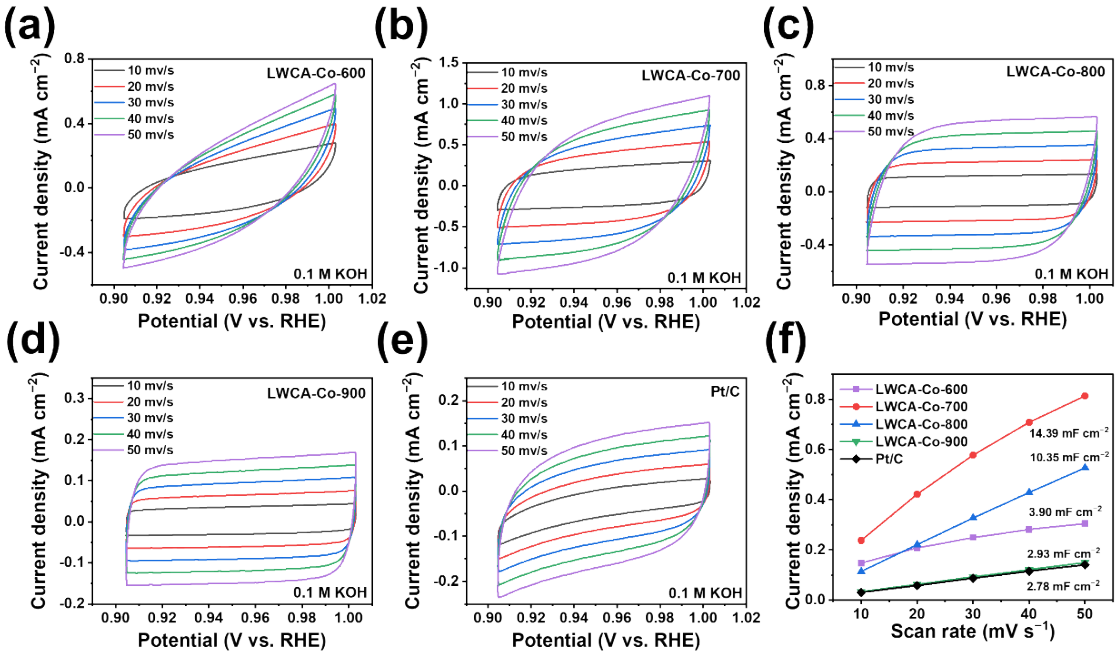

Fig. S10. CV curves with different scanning speeds of (a) LWCA-Co-600, (b) LWCA-Co-700, (c) LWCA-Co-800, (d) LWCA-Co-900, and (e) Pt/C, (f) Electrochemical double-layer capacitance values obtained from CV curves in 0.1 M KOH solution.

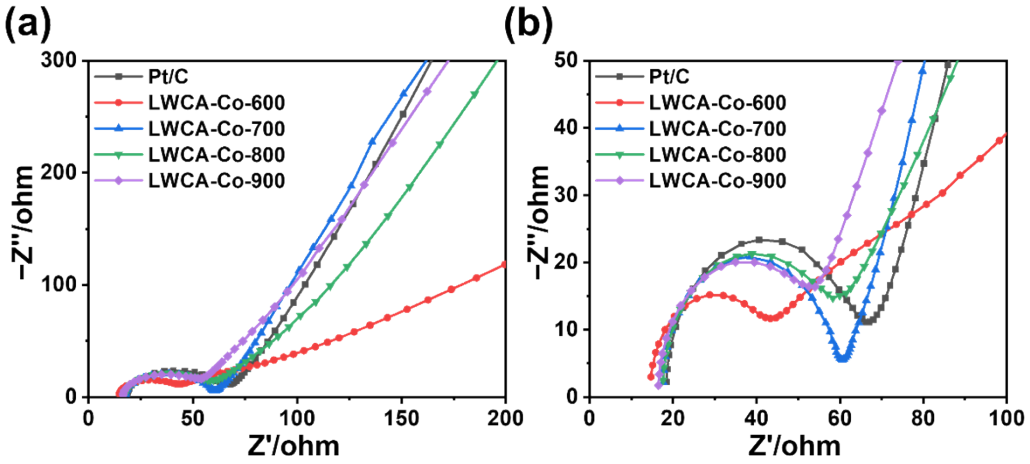

Fig. S11. (a) Electrochemical impedance spectra of LWCA-Co-600, LWCA-Co-700, LWCA-Co-800, LWCA-Co-900 and Pt/C, and (b) amplified images.

We compared the materials before and after the reaction using X-ray diffraction (XRD) analysis. The results are presented in FigS12. The prominent peak at 25° primarily arises from carbon paper. The noteworthy observation is that following the OER test, the characteristic peaks of Prussian blue analogues in the material did not completely vanish but rather persisted, indicating that there were no significant alterations to its structure. In addition, SEM images were taken of the materials before and after OER reaction in FigS13, and we could see that there was no significant change in the morphology of the catalyst before and after the reaction. It is noteworthy that the

catalyst exhibits the formation of attachments after the OER reaction, which is presumably due to the production of certain intermediates during the battery reaction process. However, in comparison to the pre-reaction material, a multitude of new peaks emerged in the material following the OER test. Despite thorough comparison with XRD database, no matching substance was identified. We speculate that the newly emerging peak is caused by the oxygen evolution reaction (OER) occurring on the positive electrode catalyst during the charging process. During charging, the surface of the positive electrode catalyst adsorbs and reacts with various substances, including ions in the electrolyte and possible reaction intermediates. This also corresponds to the attachments observed by SEM.

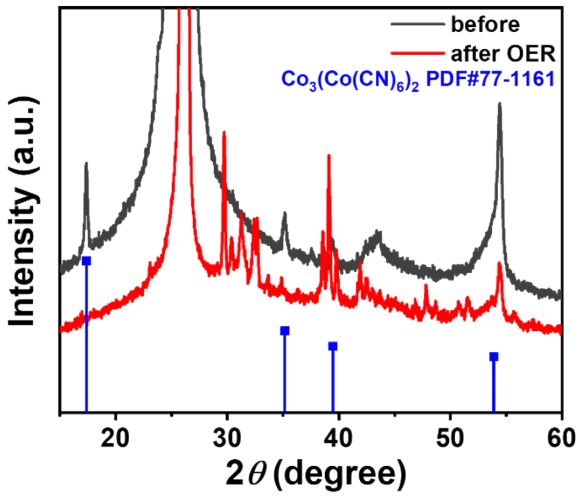

Fig. S12. Comparison of XRD Patterns of LWCA-Co-700 Before and After OER Reaction

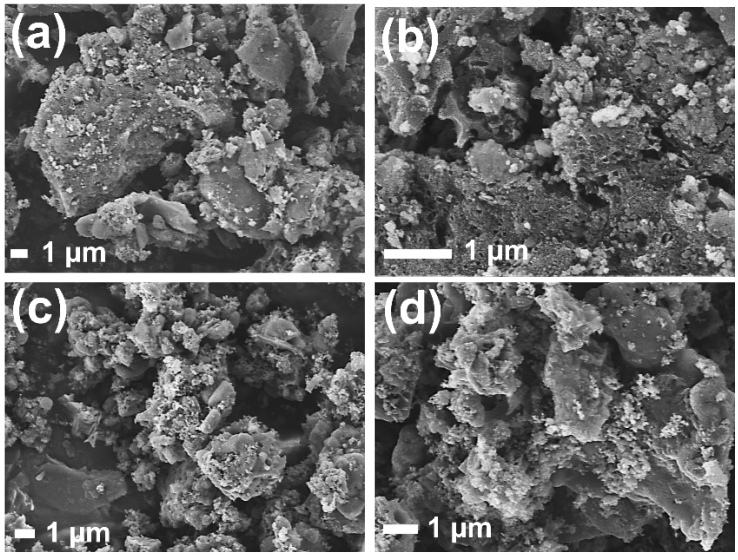

Fig. S13. SEM images of LWCA-Co-700: (a) (b) before OER Reaction, (c) (d) after OER Reaction